Design of the permanent magnet system for NIST-4

Stephan Schlamminger, *Member, IEEE*,

***Abstract*—A new watt balance, NIST-4, is currently being designed at the National Institute of Standards and Technology. This apparatus will be used to realize the unit of mass after the redefinition of the kilogram has taken effect. In order to ensure smooth operation at regular mass realizations, the watt balance should be easy to use and reliable. To meet these requirements, a permanent magnet system will be implemented to generate the magnetic flux required to operate NIST-4. A brief overview of the permanent magnet system and its design considerations are given.**

I. Introduction

NIST-4 is a next-generation watt balance currently under construction at the National Institute of Standards and Technology (NIST). The purpose of NIST-4 is to realize the unit of mass once the redefinition of the kilogram has taken effect.

A watt balance experiment is an alternating series of two measurement modes: the force mode and the velocity mode. In the force mode, a current, I, is passed through a coil with wire length l that is immersed in a magnetic field with flux density B and the resultant force on the coil is equal to the weight of a mass, $F = gm$. In the velocity mode, the same coil is moved through the magnetic field with velocity v while the induced voltage, U, is measured. If the system is aligned correctly the ratio of force to current equals the ratio of voltage to velocity. Both ratios equal the flux density integral, i.e.,

$$\frac{F}{I} = \frac{U}{v} = Bl. \tag{1}$$

The magnetic field is an essential part of a watt balance and its stability and susceptibility to systematic effects are major determinants of the precision of the balance. It is especially important that the magnetic flux density at the position of the coil is independent of the current in the coil, i.e., the current in the coil has minimal back action on the magnet.

II. Design requirements, options, and choices

Before discussing the magnet, the design specifications of the watt balance should be stated: NIST-4 is being designed to realize the unit of mass. Ideally, this realization should be performed with a minimum of personnel and cost. In order to achieve these goals, the balance must be easy to use and reliable, i.e., of low maintenance. In selecting a magnet, the practical requirements (ease-of-use, low maintenance) and the technical requirements (minimal back-action, stability of the field) should be considered.

Six different types of magnet can be used to generate a magnetic field: a conventional electromagnet, a high temperature superconducting magnet, a superconducting magnet, a permanent magnet with yokes, a yoke-less permanent magnet, or a hybrid magnet that combines any of the above. Each of the different magnet types has advantages and disadvantages. For example, electromagnets produce fields that can be varied. This includes reversing the field and turning the magnet off. In addition, the flux density produced by yoke-less electromagnets can be calculated from the known current distribution. However, electromagnets at room temperature do not provide enough magnetic flux for a precise watt balance at the kilogram level and both superconducting options add considerable complexity and cost to a watt balance.

Permanent magnets offer an economical and reliable way to generate magnetic flux densities up to ≈ 1 T. However, the magnetic flux density is fixed. One concern that is inherent to all types of magnet systems is the effect of the current during the force mode on the magnetic field. This back-action can alter the magnetic field and give raise to systematic errors. In permanent magnet systems the back-action is caused by thermal and magnetic effects. For magnets with yokes, non-linear and/or hysteresis effects in the yoke material, which is often soft iron, may additionally lead to systematic effects.

A good temporal stability of the field is necessary for watt balance experiments. The field stability of an electromagnet is determined by the stability of the field generating current. The field stability of a permanent magnet is related to the magnet's temperature. Both parameters can be stabilized with sufficient effort, but neither solution offers a clear advantage.

In the end, due to limitations in field strength, complexity, and cost, designs using electromagnets and superconductors were eliminated [1]. We believe that the possible systematic effects that arise using a permanent magnet can be sufficiently understood to build a watt balance. Although the magnetic field cannot be varied as readily as the field of an electromagnet, the magnet presented below has a yoke that allows the magnet to be operated in an "open" state and a "closed" state. The magnetic fields of the two states are different, hence with this magnet we are not limited to a single magnetic field configuration. We conclude that a permanent magnet with yoke is the most practical solution for a watt balance realizing the kilogram.

Manuscript received July 2nd, 2012.

S. Schlamminger is with the National Institute of Standards and Technology, 100 Bureau Drive, Gaithersburg, MD 20899. Phone: +1 301 975 6644, e-mail: stephan.schlamminger@nist.gov

Publisher Item Identifier S 0018–9456(97)09426–6.

Once the type of magnet has been selected, choices regarding the geometry and symmetry of the magnetic field must be made. Olsen [2] recognized the advantage of a magnetic flux density that is proportional to $1/r$. In this case, the line integral, Bl, is independent of the radius of the moving coil. This eliminates systematic effects associated with geometry changes of the coil caused by ohmic heating in the force mode.

Designing a magnet with an up-down symmetry, i.e., a mirror plane in the center, offers another advantage: The derivative of the radial field with respect to the vertical position vanishes in the symmetry plane. Therefore, the measurement uncertainty of the coil's position during force mode has a negligible contribution to the overall uncertainty.

Finally, a decision on the strength of the magnetic field and the coil radius has to be made. The following paragraphs describe an argument to determine the size of Bl for a watt balance with given parameters. This is a practical guideline rather than an exhaustive theoretical model.

During velocity mode the geometry factor, Bl, is obtained via

$$Bl = \frac{U}{v} \tag{2}$$

With standard uncertainty propagation we obtain for the relative uncertainty

$$\frac{\sigma_{Bl}^2}{B^2 l^2} = \frac{\sigma_v^2}{v^2} + \frac{\sigma_U^2}{B^2 l^2 v^2}, \tag{3}$$

where U was replaced by Blv in the last term. Once the geometry factor is known, the mass can be determined using

$$m = \frac{I}{g} Bl, \tag{4}$$

where $I = V/R$ is typically measured as a voltage drop V over a resistor, R. The relative uncertainty squared of the mass measurement is again obtained by standard uncertainty propagation:

$$\frac{\sigma_m^2}{m^2} = \frac{\sigma_V^2 B^2 l^2}{R^2 m^2 g^2} + \frac{\sigma_R^2}{R^2} + \frac{\sigma_g^2}{g^2} + \frac{\sigma_v^2}{v^2} + \frac{\sigma_U^2}{B^2 l^2 v^2}. \tag{5}$$

The geometry factor appears in the numerator in the first term and in the denominator in the last term. The first term is from the voltage measurement during the force mode. Minimizing this uncertainty requires a small Bl that correspond to a large current, which is easier to measure in relative terms. On the other hand, during the velocity mode (last term) a large Bl is advantageous since it yields a larger induced voltage, which can be measured more precisely in relative terms. These competing considerations drive the choice of Bl and, based on the above equation, an optimal value for Bl must exist.

The optimal value of Bl depends on the values of the other parameters, m, R, and v. The values from the existing watt balance, NIST-3, can be used as a first estimate. They are $v = 2$ mm/s and $R = 100\,\Omega$. It is further assumed that the voltages can be measured with an absolute uncertainty of 1 nV and that the combined contributions of the terms in the middle is 2×10^{-8}. For these assumptions, the relative uncertainty in the mass determination is shown in Fig.1. We have not included other possible uncertainties encountered in watt balance experiments. For example, the uncertainties associated with the mass transfer from vacuum to air have been ignored. However, this analysis provides a useful estimate of the minimum possible uncertainty in a watt balance based on the above assumptions as a function of Bl.

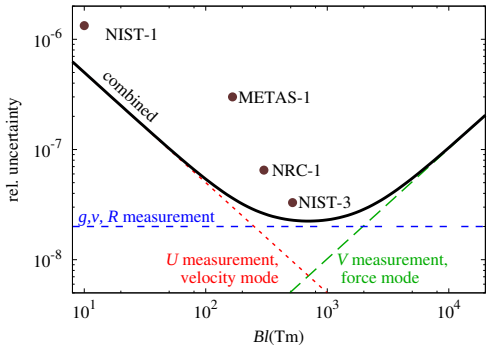

Fig. 1. Relative uncertainty of a mass realization with a watt balance as a function of the geometry factor, Bl. The thick black line indicates the combined uncertainty. The long dashed line depicts the contribution of the voltage measurement during the force mode. The dotted line gives the voltage measurement during the velocity mode. The points indicate the Bl and the relative uncertainty of recent watt balance experiments. The labels are associated with the references as follows: NIST-1:[3], METAS-1:[4], NRC-1:[5], and NIST-3:[6].

As shown in Fig. 1, the minimum uncertainty in the mass measurement is achieved at $Bl = 700$ Tm. The flux density required to meet this specification depends on the size of the moving coil. In designing NIST-4, we strive to build an apparatus that is more compact than the existing NIST-3 watt balance. The moving coil in NIST-3 has a diameter of 70 cm and about 2400 turns, which makes the coil heavy, about 23 kg. NIST-4 will have a smaller coil with a diameter of 43 cm and 1000 turns, which still requires about 1.3 km of wire. These specifications call for a magnetic flux density above 0.5 T which can be easily achieved with modern permanent magnet materials such as SmCo or NdFeB.

III. The magnetic circuit

Figure 2 shows a cross sectional view of the magnetic circuit. The magnet is rotationally symmetric about the vertical dashed line and up-down symmetric about the r-plane. Eight components, indicated by the encircled numbers, comprise the magnetic circuit. Components not relevant to the magnetic circuits, i.e., fasteners are not shown.

The magnetic flux is generated by two opposing magnet rings, parts 4 and 8. The flux lines originating from one magnet ring cannot cross those originating from the other and thus are displaced through the air gap to return to each ring. In principle, this configuration is the same as in

the previous NIST watt balance, with the two differences: (1) the source of the magnetic field is a permanent magnet and (2) the yokes guide the flux to the air gap to ensure that the flux density is proportional to $1/r$ inside the air gap. In NIST-3, the sources of the field are two superconducting solenoids whose geometrical dimensions are chosen such that the radial flux density is proportional to $1/r$ in a small volume around the coil position in the force mode. The BIPM group was first to design a permanent magnet with symmetric opposing magnets for a watt balance [7]. The magnet shown here is a variation of the BIPM design with two notable differences: The magnet is completely up-down symmetric and the magnet can be separated into two magnet systems, one much larger than the other.

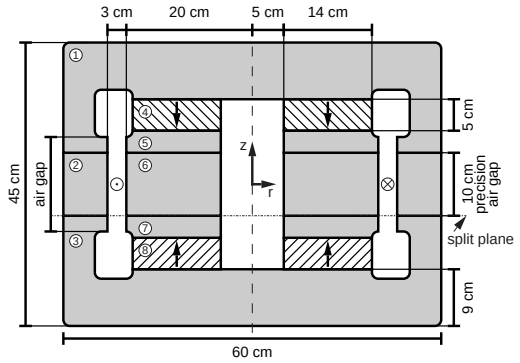

Fig. 2. Cross sectional view of the magnet system. The assembly exhibits azimuthal and up-down symmetry. The encircled numbers denote the individual components. The circles in the precision air gap indicate the current in the moving coil. The arrows in components 4 and 8 indicate the direction of magnetization.

The magnetic circuit and hence the magnetic field are perfectly up-down symmetric. This symmetry ensures a flat field profile in the center. Figure 3 shows the calculated field profile at the middle of the gap as a function of vertical position. It can be seen that the relative variation of field is smaller than 10^{-4} over 8 cm in the center of the gap.

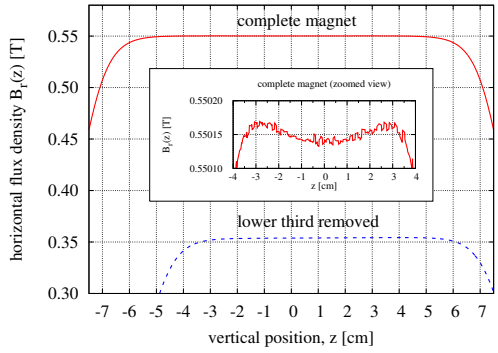

Fig. 3. The magnetic flux density in the center of the air gap as a function of vertical position. The solid line indicates the field for the closed magnet and the dashed line indicates the field in the open configuration. The inset is a zoomed view of the field in the inner most 8 cm where the field is uniform to within ±0.01 %.

Ignoring the 24 holes in the top and bottom surface of the magnet, the air gap is completely enclosed in iron, thereby shielding the moving coil from ambient magnetic fields. However, the magnet must be opened in order to insert the moving coil. The magnet will open such that the top two thirds of the magnet stay together when the bottom third is separated, as indicated by the dashed line, labeled split plane, in Fig. 2. Choosing the position of the split plane is a compromise between minimizing the force required to open the magnet and keeping the field homogeneous at the mid-plane. Opening the magnet in the mid plane requires the smallest force; opening the magnet just above the magnet rings requires the largest. However, placing the split plane in the mid-plane would compromise the field homogeneity where it is most important and placing it just above the magnet rings would expose the brittle permanent magnet material. The split plane was chosen such that the iron pieces adjacent to the gap are contiguous for the innermost 10 cm of the gap. For this design, the force required to split the magnet is about 4.7 kN. The force is attractive for small separation, it drops to zero at a separation of about 7 mm, and is repulsive for larger separations.

The possibility to open the magnet is a necessity but also a useful feature since the watt balance can function with the top two thirds of the magnet. This is useful in two ways: (1) During the early stages of experimentation frequent access to the coil is required, for example to tweak the mass distribution. In the open magnet the coil can be accessed by simply lowering the coil below components 2 and 6. (2) A frequently cited disadvantage of permanent magnet systems is that the field is fixed. However, this magnet allows operation at two different field strengths, albeit with lesser homogeneity in the open configuration. As shown in Fig. 3, the radial field in the open configuration is about 65 % of the field in the closed configuration.

The yoke is made from low carbon steel (A36) and the permanent magnets from Sm_2Co_{17}. The outer diameter of the magnet is 60 cm with a height of 45 cm. The total mass of the magnet system is 850 kg.

IV. Calculating the magnetic circuit with an analytic approximation

Typically, permanent magnet systems are designed using finite element analysis (FEA) software. While we employed FEA software, we have also used a simplified analytical model for guidance. Significantly less time consuming than full FEA analysis, the model allowed for much faster parameter variations to optimize the magnitude of the flux density. The approximation provides insight into the physical nature of systematic effects of using permanent magnet systems in watt balances. FEA programs can be employed to calculate the size of systematic effects, but generally do not provide insight into the physical causes of these effects.

An analytical calculation is possible because rare earth magnets have a linear recoil curve, see Fig. 4. The relationship between the magnetic flux density, B_m, and the magnetic field, H_m, in the magnet in the second quadrant is approximately linear, $B_m(H_m) \approx B_r + \frac{B_r}{H_c} H_m =$

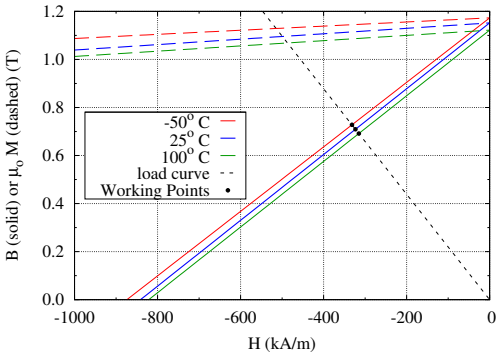

Fig. 4. Recoil curve (solid) and magnetization curve (dashed) of SmCo in the second quadrant.

$B_r + \mu_r \mu_o H_m$, where B_r is the remanence, H_c is the coercive field, and μ_r the recoil permeability. The magnetic circuit can be solved analytically using the recoil curve and three additional assumptions: (1) The yoke is a perfect conductor of the magnetic flux. (2) Stray flux is neglected. (3) The magnetic field in the gap can be calculated by considering one half of the magnet. Assumption one is reasonable if the iron is far from saturation, which is the case in the magnet shown here. Assumption three is valid since the flux in the other half of the magnet prohibits flux leakage over the mid plane. With these assumptions, the analytic field calculation will be less accurate but the results should not differ by more than 10%.

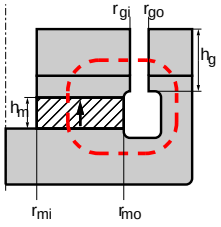

Fig. 5. The bottom quarter of the magnet, which has rotational symmetry around the dashed dotted line. The thick dashed line indicates the integration path for Ampere's law.

There are three unknowns in the magnetic circuit, the flux density in the magnet B_m, the flux density in the air gap B_g, and the magnetic field in the magnet, H_m, calling for three equations: the recoil curve, Ampere's law, and flux conservation. Ampere's law is evaluated along the path indicated in Fig. 5 . The field in the gap is given by $H(r) = 1/\mu_o B_g r_{gi}/r$, where B_g is the magnetic flux density at the inside edge of the gap. With this expression, Ampere's law gives $H_m h_m + B_g/\mu_o r_{gi} \ln(r_{go}/r_{gi}) = 0$. The flux conservation can be written as $B_m(r_{mo}^2 - r_{mi}^2)\pi = B_g 2\pi r_{gi} h_g$. The solutions for the three parameters are

$$H_m = -\frac{B_r r_{gi}(r_{mo}^2 - r_{mi}^2)\ln\frac{r_{go}}{r_{gi}}}{\mu_o D}, \tag{6}$$

$$B_m = \frac{2B_r h_g h_m r_{gi}}{D}, \text{ and} \tag{7}$$

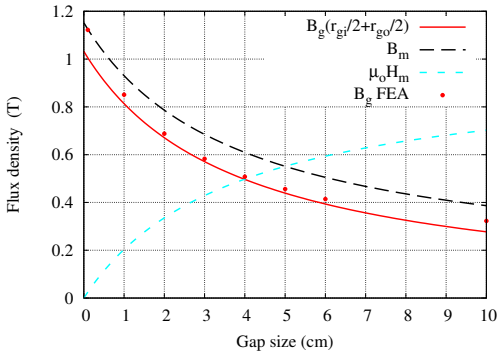

Fig. 6. The field in the center of the air gap (solid line) as a function of air-gap size. For this calculation, the inner radius of the gap, r_{gi}, was held constant at 20 cm. The dots indicate results from a FEA calculation.

$$B_g = \frac{B_r h_m (r_{mo}^2 - r_{mi}^2)}{D}, \text{ with} \tag{8}$$

$$D = 2 r_{gi} h_g h_m + r_{gi}\left(r_{mo}^2 - r_{mi}^2\right)\mu_r \ln\frac{r_{go}}{r_{gi}}. \tag{9}$$

The results of these equations as a function of gap size, $r_{go} - r_{gi}$ is shown in Fig. 6 together with the results from the FEA calculation. The analytical solution gives a good, but not perfect, approximation of the field in the gap. The calculation can be improved by adding fringe fields. A detailed analysis of the fringe fields is outside the scope of this article. Equations for estimating the fringe fields can be found in [9].

V. Estimate of systematic effects

Moving from a watt balance (NIST-3) with a superconductor to one (NIST-4) with a permanent magnet requires careful assessment of the systematic effects intrinsic to permanent magnet systems. A leading cause of systematic effects is the current in the coil during the force mode altering the magnetic flux generated by the permanent magnet. In this case, the Bl in the velocity mode differs from the Bl in the force mode, violating the basic assumption of the watt balance and therefore causing a systematic shift in the result. This back-action on the magnet due to the current in the force mode can be caused by either thermal or the magnetic effects.

A. Thermal effects

Temperature changes affect the permanent magnet through three mechanisms: (1) The recoil curve changes as a function of temperature, (2) The geometry changes as a function of temperature, e.g., the gap width increases with higher temperature, and (3) The reluctance of the yoke increases with increasing temperature.

(1) The effect of temperature changes on the permanent-magnet material can be understood by examining Fig. 4. For higher temperatures, the recoil curve shifts closer to the origin while the load line stays constant resulting in a smaller B_m. Note that B_g is proportional to B_m due to flux conservation. The recoil permeability is nearly independent of temperature while the remanence is a linear

function of temperature, $B_r(T) = B_r(T_o)\,(1+\alpha(T-T_o))$, with $\alpha \approx -300\times10^{-6}\,\mathrm{K}^{-1}$. In this approximation, α is the relative change of the magnetic field in the air gap. This effect can be minimized by (a) choosing a different grade of permanent magnet material or (b) controlling the temperature of the magnet. It is possible to use a permanent magnet material with a much lower temperature coefficient, e.g., alloying SmCo with Gd results in $\alpha \approx -10\times10^{-6}$. However, these materials come at higher cost and/or lower B_r and, as shown below, the temperature change of this magnet is not a concern. The normal grade Sm_2Co_{17} was deemed sufficient for this application.

(2) Increasing the magnet's temperature will cause expansion of the yoke and hence increase the width of the air gap inside the magnet. The linear expansion coefficient of low carbon steel is $12\times10^{-6}\,\mathrm{K}^{-1}$. The analytic approximation in the previous section yields a relative effect of thermal expansion of $\Delta B_g/B = -4.5\times10^{-6}\,\mathrm{K}^{-1}$.

(3) The magnetic permeability of the yoke decreases with increasing temperature, yielding a larger reluctance. As a consequence, the demagnetizing field in the yoke is larger at higher temperatures and a larger fraction of the field goes into the fringe fields. Since the fringe fields carry less than 10% of the flux and the Curie Temperature of Fe is higher than that of SmCo, the size of this effect is negligible compared to the effect due to the temperature coefficient of SmCo.

The leading thermal effect is the dependence of the remanence on the temperature of the magnet. However, thermal effects are reduced by the large heat capacitance of the magnet, $C = 4\times10^5$ J/K, and the fact that the magnet is in vacuum. The support structure, currently under consideration, provides a heat conductance of 4 W/K, leading to a thermal time constant of more than 8 d. The dissipated power in the moving coil is proportional to the resistance of the moving coil, i.e., inversely proportional to the copper mass. Since the current during the force mode and the number of turns is given by the design, i.e., $Bl = 700$ Tm and m=1 kg the only free parameter is the wire diameter. For reasonable wire gages (AWG-19 through AWG-29) the dissipated power in the force mode ranges between 1.8 mW and 18 mW. Note, in order to build a 1 kg watt balance, only a force that correspond to 500 g mass needs to be generated, see [8] for details. Assuming these power levels, and the velocity and the force-mode measurements each lasts 10 minutes, the temperature modulation of the magnet is between 1.4 μK and 14 μK producing a relative systematic effect of at most 5×10^{-9}. This systematic effect can be further decreased by adding a non-inductive heater to the magnet. This heater would turn on during the velocity mode with a power level similar to that of the dissipation in the force mode.

As shown above, a uniform temperature change caused by the current in the force mode is not a concern. However, local heating effects could change the reluctance of the yoke at the coil position and divert a fraction of the flux around the coil. This effect is currently under investigation. To mitigate this effect, an option to install copper sheets to spread the heat uniformly over the soft iron on both sides of the air gap is included in the magnet design.

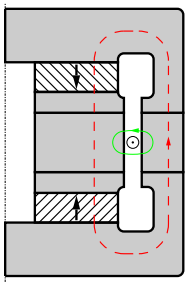

Fig. 7. Current in the moving coil, indicated by the circle in the gap, drives flux through the magnet. Flux lines similar to the solid line give rise to the reluctance force. The dashed line is an example of a flux line that contributes to the demagnetization.

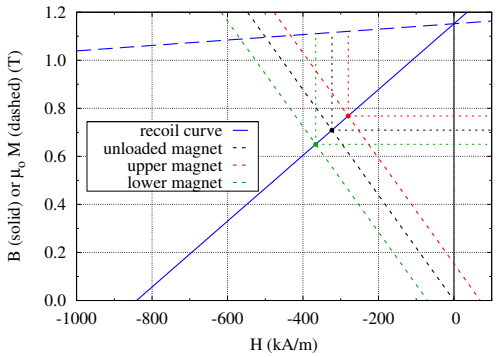

Fig. 8. The recoil curve of SmCo at room temperature with three load curves corresponding to three different currents in the moving coil. From the left: the magnetic field generated by the moving coil anti-parallel, zero, or parallel to the magnetization of the SmCo ring. The horizontal offset of the load curves is ±70 kA/m, a field that is about 1000 times larger than that expected during force mode.

B. Magnetic effects

Figure 7 shows schematically two flux lines caused by current in the coil. Both types of flux lines will affect the watt balance experiment. Flux lines similar to the dashed line will strengthen/weaken the magnetization of the top/bottom SmCo ring. The other type of flux line produces a force on the coil toward the center of the magnet. This force is called the reluctance force.

Integrating H along the dashed line in Fig. 7 no longer yields zero, but NI, where N is the number of turns and I is the current in the moving coil. In the analytical model, adding this additional magnetic field corresponds to the shifting of the load line as shown in Figure 8. In the NIST-4 magnet, the additional magnetic field is parallel to one magnet ring and anti-parallel to the other. Hence the flux from one magnet increases while the flux from the other decreases. Since the center yoke spreads the flux, the flux density in the gap is, to first order, unchanged. This compensation is intrinsic to the symmetric design with oposing magnets and one of the reasons it was chosen.

The reluctance force acts independently of the direction of the current in the coil. Its direction always points from the coil to the center of the magnet system. When the coil

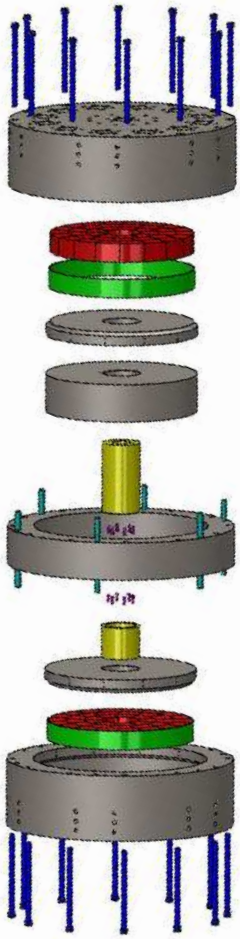

Fig. 9. Exploded view of the magnet. Yoke parts are drawn in gray and permanent magnets in red. Each SmCo ring is comprised of 40 magnetic wedges. The golden sleeves are made from stainless steel and their purpose is to center the inner yokes and the magnet rings on the outer yoke pieces. Dowel pins, drawn in cyan, align the three parts of the outer yoke to each other.

is in the center, the energy stored in the magnetic field in the gap is minimal. The force is the negative derivative of the energy with respect to the position. The reluctance force can be determined with an analytical approximation or with a FEA calculation. The approximation yields

$$F \approx -\frac{2\pi\mu_o N^2 I^2 1/2r_{gi} + r_{go})z}{2h_g(r_{go} - r_{gi})}, \qquad (10)$$

where z denotes the vertical position of the coil. Note that to be consistent, $2h_g$ is the full height of the air gap, i.e. 15 cm. A coil with $N = 1000$ turns carrying a current of 7 mA experiences a force of 18.5×10^{-6} N/mm. Since in a watt balance experiment the force difference between two different current directions, i.e., +7 mA and −7 mA is measured; only a position change of the coil in the two modes will cause a systematic effect. In order to keep the relative contribution of the reluctance effect below 10^{-8} on a 1 kg mass, the position of the coil cannot be different by more than 5 μm for the two current directions. In addition, the exact size of the effect can be measured and a correction can be applied.

VI. Construction of the magnet

Electron Energy Corporation (EEC)[1] has advanced the conceptual design presented in previous sections into a detailed design. NIST has approved the final drawings and EEC started the production and assembly of the magnet in June 2012.

Figure 9 shows an exploded view of the magnet. Besides the pieces that comprise the yoke (gray) and the permanent magnets (red), nonmagnetic parts are used to assemble the magnet and to register individual pieces. Dowel pins ensure a smooth opening and closing of the magnet. The SmCo rings are composed of 40 sectors which are epoxied together. A stainless steel retainer ring provides additional support against the repulsive magnetic forces between the sectors. The SmCo will not be exposed when the magnet is opened. Once the magnets are mounted between the yoke pieces, a stable configuration is reached.

The magnet is expected to arrive at NIST, Gaithersburg in the spring of 2013. In the meantime, preparations are being made for the installation of the vacuum vessel housing the NIST-4 watt balance.

VII. Summary

This article reviews considerations leading to the design of the permanent magnet for NIST-4. A permanent magnet is deemed to be the most reliable and cost effective approach for a watt balance realizing the kilogram. Considerations regarding the strength of the fields were discussed. An analytic approximation allowing to estimate the systematic effects associated with a permanent-magnet system was introduced.

References

[1] S. Schlamminger, "The Permanent Magnet System for NIST-4", CPEM-2012 Digest, CPEM 2012, pp. xxx, July 2012.

[2] P.T. Olsen, W.D. Phillips, and E.R. Williams, "A Proposed Coil System for the Improved Realization of the Absolute Ampere", *J. Res. Nat. Bur. Std.*, vol. 85, no. 4, pp. 257-272 July/August 1980.

[3] P.T. Olsen *et. al*, "A Measurement of the NBS Electrical Watt in SI Units",*IEEE Trans. Instrum. Meas.*, vol. 38, no. 2, pp. 238-244, April 1989.

[4] A. Eichenberger, *et. al*, "Determination of the Planck constant with the METAS watt balance", *Metrologia*, vol. 48, pp. 133-141, March 2011.

[5] A.G. Steele *et al*, "Reconciling Planck constant determinations via watt balance and enriched-silicon measurements at NRC Canada", *Metrologia* vol. 49, L8-L10, January 2012.

[6] R.L. Steiner *et. al*, "Uncertainty Improvements of the NIST Electronic Kilogram", *IEEE Trans. Instrum. Meas.*, vol. 56, no. 2, pp. 592-595, April 2007.

[7] A. Picard et al., "The BIPM Watt Balance", *IEEE Trans. Instrum. Meas.*, vol 56, no 2, 538542, April 2007.

[8] R.L. Steiner *et. al*, "Towards and electronic kilogram: an improved measurement of the Planck constant and electron mass",*Metrologia* vol. 42, p. 431-441, September 2005.

[9] H.A. Leupold and E. Potenziani II, "A Permanent Magnet Circuit Design Primer", Army Research Laboratory, ARL-TR-946, `www.dtic.mil/cgi-bin/GetTRDoc?AD=ADA311457`

[1] Certain commercial equipment, instruments, or materials are identified in this paper in order to specify the experimental procedure adequately. Such identification is not intended to imply recommendation or endorsement by the National Institute of Standards and Technology, nor is it intended to imply that the materials or equipment identified are necessarily the best available for the purpose

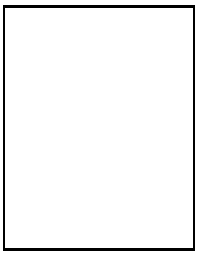

Stephan Schlamminger (M'12) was born in Kelheim, Germany. He received a diploma in physics from the University of Regensburg in 1998, and a Ph.D. degree in experimental physics from the University of Zurich, Switzerland in 2002. From 2002 to 2010 he worked at the University of Washington on an experimental test of the equivalence principle. He is currently with the National Institute of Standards and Technology, where he is working on the watt balances NIST-3 and NIST-4.